

General Keplerian Dynamics (GKD): A Testable Grand Unified Theory

Brent Lee Jarvis

CEO, Galaxytech

Abstract. Newton generalized Kepler's laws of planetary motion when he developed his laws of Universal gravitation. Additional generalizations are submitted and an auspicious unified model that can be tested experimentally is disclosed.

1. Introduction

Due to a special relativistic principle referred to as volume dependent angular momentum (VDAM), it will be shown that the gravitomagnetic force is exponentially greater than currently assumed. A common example that demonstrates the VDAM principle is a mountain. From your frame of reference, a mountain seems as though it is at rest, but its relative velocity is $\approx 1,000$ mph as the Earth spins on its axis (assuming the mountain is located on the Earth's equator). From a solar frame of reference, its relative velocity is $\approx 67,100 \pm 1,000$ mph. The greater the volume of the inertial coordinate system, the greater the relative velocity of the mountain.

Since gravity is only dependent upon the *inertial mass* of a body according to the equivalence principle of general relativity, and not its *relative motion* (i.e. its *relativistic mass* in special relativity), the “dark matter” hypothesis is needed to explain the dynamics of galactic systems. When a galaxy's gravitomagnetic (GM) field is determined from Hubble's volume, the VDAM of the galaxy completely eliminates the necessity of dark matter (the Hubble volume also establishes a macro-cosmic limit for the correspondence principle):

$$[1] \mathbf{B}_g = \frac{G \mathbf{L}_D}{2c^2 r^3} \propto \mathbf{V}_H = \left(\frac{c}{H_0}\right)^3$$

where \mathbf{B}_g is the gravitomagnetic (GM) field, \mathbf{L}_D is the volume dependent angular momentum (VDAM) of the galaxy, G is the gravitational constant, c is the velocity of light in a vacuum, r is a galaxy's radius, \mathbf{V}_H is the Hubble volume, and H_0 is Hubble's constant. The consistency in the rotation speeds of stellar systems, independent of their distance from galactic nuclei, is simply due to the conservation law of angular momentum. The “dark matter” of a galaxy is equivalent to the special relativistic mass-energy of its GM field^[1].

2. A Generalized 1st Law of Universal Motion (GKD1)

Newton's generalization of Kepler's 1st law of planetary motion can be stated as: The shape of a secondary's orbit is a conic section with the center of mass (COM) at one foci.

GKD1 synthesizes the conic section of a secondary with its orbital inclination via a toroidal reference frame embedded within an inertial Cartesian coordinate system. GKD1 can be stated as: The shape of a secondary's orbit traces the surface area of a torus with the COM at the *origin* of the toroidal cavity.

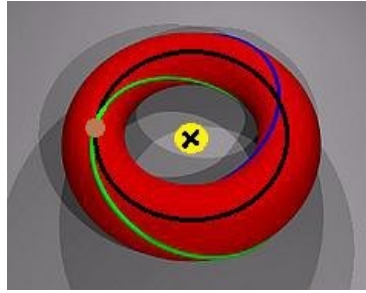


FIG. 1: Image is exaggerated. The “x” represents the center of mass (COM). The torus can be constructed from an auxiliary circle with a radius equivalent to the secondary's apoapsis distance and a minor auxiliary circle with a radius equivalent to the distance of its periapsis (relative to the COM). The radius of the coplanar orbital axis (black) is equivalent to the secondary's average true anomaly distance (equivalent to the semi-minor axis of a Keplerian ellipse). The yellow and brown dots represent a primary and secondary respectively. The blue and green paths are Villarceau circles (example orbital paths).

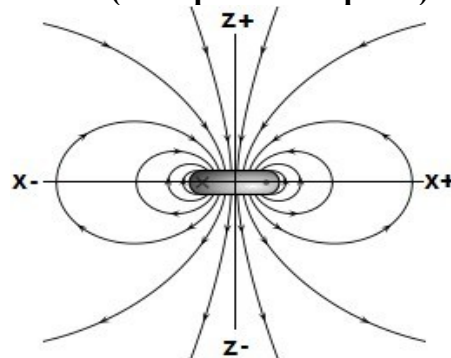


FIG. 2: An example half section of a primary's gravitomagnetic (GM) field. Conic shapes are all embedded within each quadrant of the GM lines of force.

Conic shapes (circles, ellipses, parabolas, and hyperbolas) are all embedded within each quadrant of a primary's GM field along its z -axis when the coplanar orbital axis is oriented along its x and y plane (the gravitoelectric field will be discussed in the generalized 3rd law).

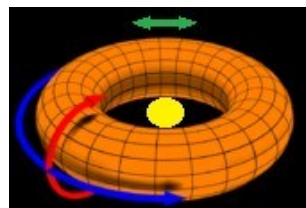


FIG. 3: Image is exaggerated. The major axis is represented by the blue vector, the minor axis is represented by the red vector, and the green pseudovector represents the eddy axis (precession).

It will be shown within the generalized 2nd law of Universal motion (GKD2) that the orbit of a secondary has three primary axes of rotation. The three axes are referred to as the major, minor, and eddy axes (precession is due to gravitoelectromagnetic (GEM) induction in GKD).

Even though an ellipse and a Villarceau circle (a slanted torus section) are geometrically equivalent relative to a two dimensional reference frame there is a subtle difference between the two in three dimensions. While an ellipse and a Villarceau circle both trace the oscillatory cycle of a secondary's apoapsis and periapsis relative to the COM, a Villarceau circle also traces an additional cycle which is perpendicular to the coplanar orbital axis. The additional cycle contains two reference points that are referred to as the crest and trough, in which the crest is perpendicular to the coplanar axis in the northernmost polar direction. The distance between the crest or trough from the coplanar axis is referred to as the orbital amplitude.

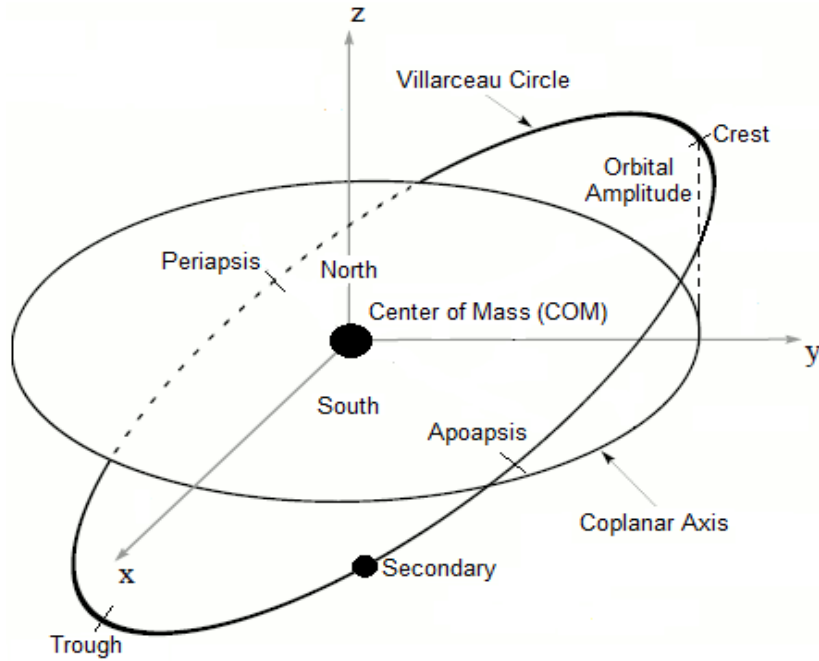


FIG. 4: The basic poloidal points of reference and the orbital amplitude of a secondary's orbit.

In GKD3 there are two periods that are considered in Newton's version of Kepler's 3rd law instead of only one period. An “elliptical” orbit results from a **1:1** ratio between a secondary's major and minor periods (which is referred to as its polar frequency (**T**), being dependent upon the mass and distance of the secondary relative to the primary's mass and position). The introduction of the polar frequency term procures orbital paths that are not limited to conic sections. Geological evidence^[2] indicates a **4:1** polar frequency for our solar system's orbit.

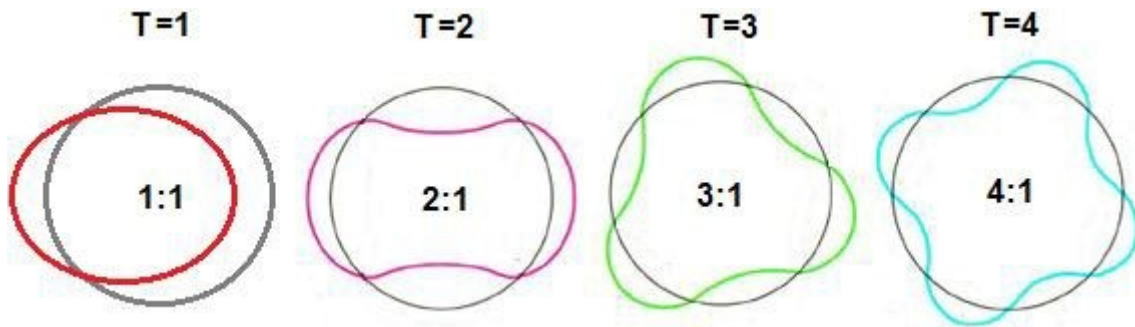


FIG. 5: Stellar orbital paths relative to galactic nuclei are not limited to conic sections according to the formalism of GKD3 (analogous to the de Broglie matter-waves of quantum mechanics).

3. A Generalized 2nd Law of Universal Motion (GKD2)

Kepler's 2nd law of planetary motion can be stated as: A line joining a planet and the Sun sweeps out equal areas during equal intervals of time.

GKD2(a) can be stated as: The radii of a secondary's major (r_1), minor (r_2), and eddy (r_3) axes, joining the major, minor, and eddy pivots respectively, individually sweep out equal sectors during equal intervals of time.

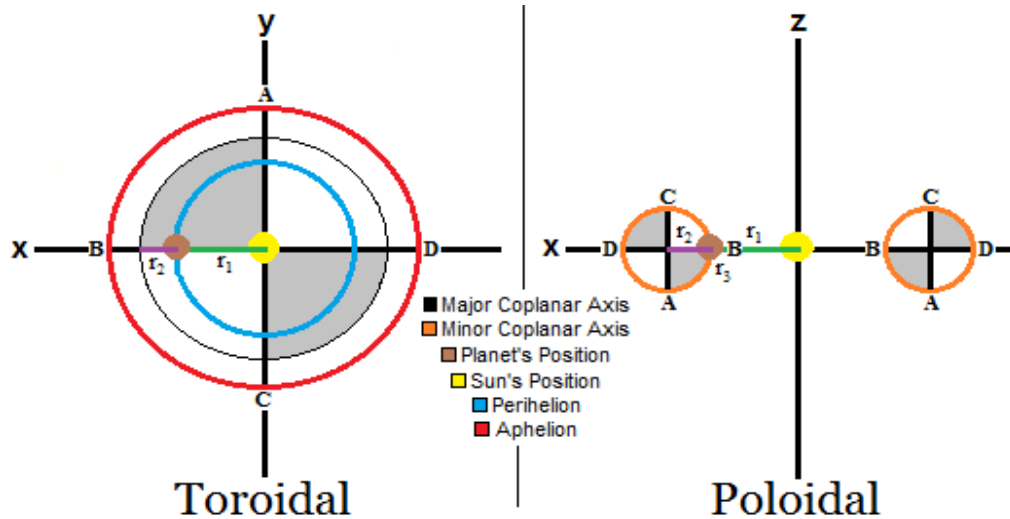


FIG. 6: Image is exaggerated. The radii r_1 and r_2 are overlapping since the planet is at perihelion. The radius of the eddy axis (r_3) is miniscule. The planet orbits a perpendicular torus along the minor coplanar axis which is observed as precession (represented by the eddy axis pseudovector in FIG. 3).

GKD2(b) can be stated as: The radius of a secondary's major axis (r_1) is equivalent to the semi-minor axis of its Keplerian ellipse when unperturbed by outside GEM forces, or


$$[2] r_1 = b = a\sqrt{1-e^2},$$

where b is the semi-minor axis, a is the semi-major axis, and e is the eccentricity of the ellipse. The radius (r_1) is also equivalent to the geometric mean of the secondary's apoapsis and periapsis distances relative to the major pivot (barycenter), or

$$[3] r_1 = \sqrt{r_{\min}r_{\max}}$$

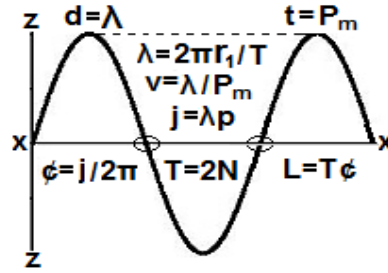
GKD2(c) can be stated as: The angle of the secondary's toroidal major axis, relative to any other plane of reference, can be determined from the angle of r_1 relative to the plane of reference when the secondary is at crest or trough (when r_2 is perpendicular to r_1 and the hypotenuse is joined by the major and eddy pivots).

GKD2(d) can be stated as: The relationship between the major axis revolution period, the minor axis revolution period, and the polar frequency of a secondary's orbit is:



$$T = \frac{P_M}{P_m}; T = 1, 2, 3, 4, n, \text{ etc.}$$

where P_M is the major period, P_m is the minor period, and T is the polar frequency. Additional GEM wave formulas are:



where λ is wavelength, v is velocity, j is an astronomical analog of Planck's proportionality constant, ϕ is the reduced constant, p is momentum (where mass is measured in Solar Mass units), L is angular momentum, N is the node quantity, d is distance in light units, and t is time in terrestrial minor periods (P_{Em}). Considering only the Sun-Earth system, the radius of the Earth's major axis (r_{E1}) relative to the Sun's COM is:

[4] $r_{E1} = \sqrt{r_{\min} r_{\max}} \approx \sqrt{(0.9832898912 \text{ AU}) (1.0167103335 \text{ AU})} \approx 0.999860486872609 \text{ AU}$, where AU is an astronomical unit. The barycenter distance can be determined by:

$$[5] r_{E1} = \frac{a}{1 + m_1 / m_2},$$

where a is the distance derived from equation [4] and m_1 and m_2 are each of their masses. Compensating for the barycenter we get $r_{E1} \approx 0.99986015 \text{ AU} \approx 149,576,950,315$ meters, which

$$[6] \frac{r_{E1}}{1 \text{ lm}} \approx 8.315583339808087 \text{ lm.}$$

can be converted into light minutes by:

$$[7] \lambda_E = \frac{2\pi r_{E1}}{2(0.5)} \approx 52.24835106131297 \text{ lm.}$$

Since the node quantity is 2 for the Earth's orbit ($T = 1$), the Earth's wavelength λ_E is

The Earth's GEM wave velocity (not its velocity relative to the Sun's position) can be determined

$$[8] v = \frac{\lambda_E}{P_m} \approx \frac{52.24835106131297 \text{ lm}}{P_{Em}}$$

from:

$$[9] j = \lambda p \approx \frac{9.4124100318113 \cdot 10^{-3} \text{ ls}^2 \cdot M_{\odot}}{P_{Em}}$$

where P_{Em} is the Earth's minor period. The velocity can then be used to deduce the astronomical analog of Planck's proportionality constant, which is approximately (on a stellar scale not a galactic scale due to VDAM):

The reduced constant is simply $j / 2\pi = \phi$. Analogous to the quantized angular momenta of atomic systems, the angular momenta of stellar systems can be quantized to:

$$[10] L = T\phi.$$

It is important to note that the minor period is measured by the amount of time that elapses between two passages of a crest, or two passages of a trough. Since the toroidal major axis radius is less than the Keplerian semi-major axis the standing wave velocity of a secondary is less than the mean velocity calculated with Kepler's version, and the GEM waves are not precisely sinusoidal for reasons that will become apparent in a moment (the GEM waves have a "root mean square" waveform).

GKD2(e) can be stated as: The minor axis is perpendicular to the major axis, and the eddy axis is perpendicular to the minor axis, when unperturbed by GEM forces. Since this is analogous to eddy currents, GKD2(e) is referred to as the eddy effect. Fractal iteration of the eddy effect is limited by the secondary's intrinsic center of mass point (see FIG. 7 on the next page).

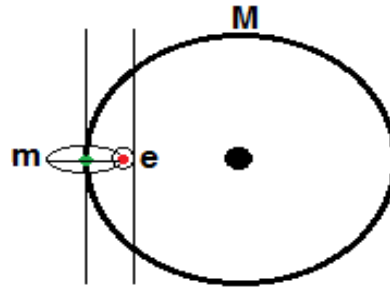


FIG. 7: Image is exaggerated. The eddy axis (e) would be miniscule. The minor axis (m) would appear as a line in 2-D. The “M” represents the major axis. The black, green, and red dots represent the major, minor, and eddy pivots respectively.

GKD2(f) can be stated as: The curl of the eddy effect obeys the right-hand rule for vector cross products relative to the secondary's “mass current” along the major axis. **The rotation vector of the minor axis has reflection symmetry along the z-axis of an inertial Cartesian coordinate system when the major axis is oriented on the x and y plane.** The pseudovector of the eddy axis is mathematically equivalent to a 3-D bivector.

The above generalizations have been consolidated into what are referred to as gyrographs, which simplify calculations pertaining to the position and/or momentum of a secondary at any given time in its orbit. The diagrams are referred to as gyrographs since all of the terms that pertain to the angular momentum of a secondary are kept constant except for the relative gyration of each axis of rotation within an inertial Cartesian coordinate system.

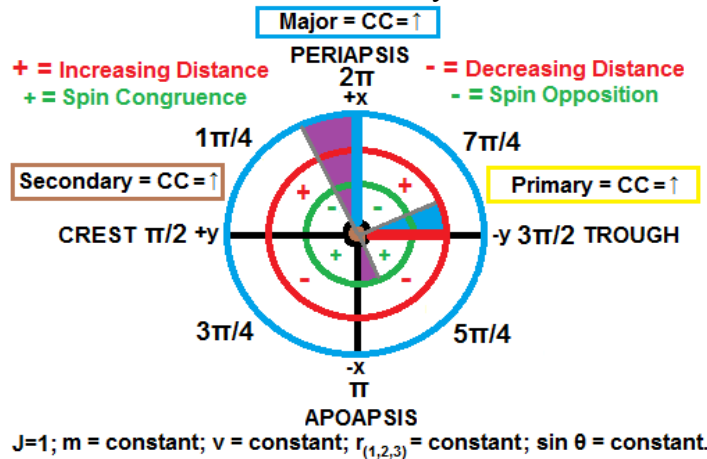


FIG. 8: Image is exaggerated. The axes of rotation are superimposed on the same plane but the gyrograph can be disassembled to determine the 3-D position of the secondary by linking the radii back together in their proper orientation (+z is coming out of the page). The radius of the major axis (blue) always defines the “time” and all three radii “tick” counter-clockwise (CC=↑) at the same rate since $J=1$. The radius r_2 is 90° out of phase with r_1 and r_3 is 90° out of phase with r_2 , 180° out of phase with r_1 . The intrinsic spin of the primary and secondary are both $CC=↑$. The rotation vector of the minor axis (red) flips signs at periapsis and apoapsis (the “+” and “-” represent the increasing (\rightarrow) and decreasing (\leftarrow) distance of the secondary's position relative to the primary's position respectively). The pseudovector of the eddy axis (green) flips signs at crest and trough (the “+” and “-” in this case represent rotation congruence (\uparrow) and opposition (\downarrow) relative to the secondary's intrinsic spin respectively).

Throughout a full revolution of a gyrograph we can see that the combined gyration of the major and eddy axes are equivalent to the intrinsic spin angular momentum of an electron:

$$[11] \mathbf{S} = \hbar \sqrt{\frac{1}{2}(\frac{1}{2}+1)},$$

where \mathbf{S} is the spin angular momentum and \hbar is the reduced Planck constant:

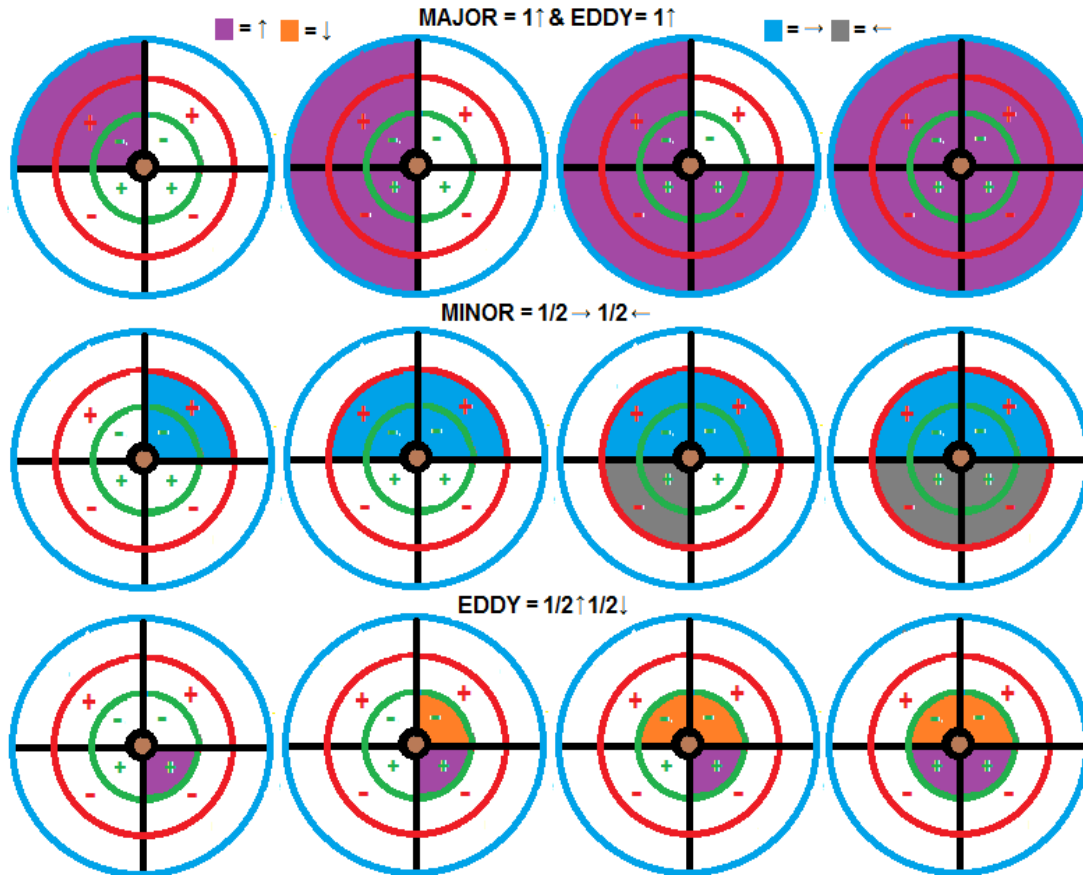


FIG. 9: A full revolution of the individual axes of rotation in a gyrograph. By precessing the gyrograph by $\frac{1}{2}\downarrow 1\frac{1}{2}\uparrow = 2\pi r_3$ per wavelength the secondary's 3-D position can be determined at any time.

The gyration of the torque axis is $\frac{1}{2}\downarrow$ and $1\frac{1}{2}\uparrow$ per wavelength. The $\frac{1}{2}\downarrow$ should not be interpreted as an alteration in the secondary's intrinsic spin orientation, but as the frame-drag (torque) per wavelength due to GEM induction. With this interpretation, the perturbations of a secondary's orbit predominately originate from the parity inversion of the eddy axis every $\frac{1}{2}$ revolution of the minor axis. There are also two types of torque that can be deduced from the gyrographs; a “boost torque” (magenta) and a “tranquil torque” (orange). Perhaps Kepler was correct and a secondary “skips” to the harmony of the spheres!

GKD2(g) can be stated as: In addition to Newton's generalization of Kepler's 2nd law, which is the conservation of angular momentum, torque is also conserved by GEM induction (experiments regarding this generalization will be discussed next).

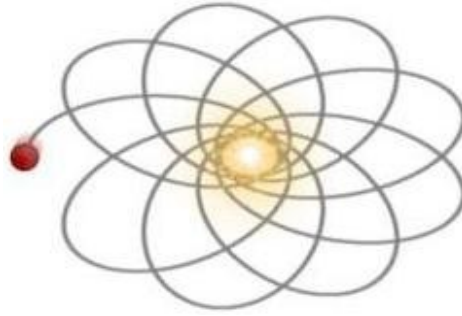


FIG. 10: Image is exaggerated. If angular momentum is constant ($L = mvr \sin \theta = \text{constant}$) then the orbital paths that resemble the “flower of life” should not be observed. Assuming torque conservation ($\Delta L / \Delta t$) amends the law of conservation of angular momentum.

Since time is intrinsically related to the Earth's rotation there is an obvious correlation between GKD and Einstein's theory of general relativity (GR). The primary difference between the two is the precession rate of an \uparrow primary \uparrow secondary system (such as the Sun-Earth system) relative to an \uparrow primary \downarrow secondary system (such as the Sun-Venus system). To the author's knowledge, there has yet to be an experiment that has tested the aphelion precession rate of Venus relative to its conventional perihelion precession. GR predicts a perihelion precession of ≈ 8.6 arc seconds per century, but the observed precession is ≈ 2.04 arc seconds per century. According to GKD, the “reverse” precession of Venus is ≈ 6.12 arc seconds per century (if the tranquil torque is 2.04 then the boost torque is 6.12).

Since there are two known spin orientations for an electron (\uparrow or \downarrow), a method to test GKD on an atomic scale may be to repeat the Hafele-Keating experiment^[3] with two atomic clocks onboard the same aircraft (one clock could have an \uparrow proton \uparrow electron hydrogen-1 (protium) orientation, and the other an \uparrow proton \downarrow electron protium orientation). Even though each clock will travel at the same relative velocity there should be a marginal difference in their electronic precession rates (assuming

the spin orientations are kept constant and the aircraft maintains an opposite flight path (for optimal results) relative to the Earth's spin). Taking the effects of GR into account, the greater the velocity of the aircraft and the lower its altitude, the greater the predicted difference between the measured times on each atomic clock.

4. A Generalized 3rd Law of Universal Motion (GKD3)

According to Kepler's 3rd law of planetary motion, the square of a secondary's orbital period is proportional to the cube of the semi-major axis of its orbit. Newton later modified this law to include the mass of each body:

$$[12] m_1 + m_2 = \frac{A^3}{P^2},$$

where m_1 and m_2 are each of their masses (in Solar Mass units), A represents the semi-major axis distance (in Astronomical Units), and P represents the period of the orbit (in Years). As was discussed previously, however, there are at least two periods which must be considered in Newton's version of Kepler's third law. Until the predictions that were discussed previously can be verified experimentally, it will be assumed equation [12] can be modified to:

$$[13] m_1 + m_2 = \frac{A^3}{TP_M^2},$$

When $T=1$, equation [13] is equivalent to Newton's generalization, but introducing the polar frequency term geometrically enables orbital paths that are not limited to conic sections. With this interpretation, the consistency of a star's rotation speed independent of its distance from the galactic nucleus would be expected, so long as the value of T increases as the star's distance increases (which can also be experimentally investigated). Current estimates for our solar system's major period range from **225-250 Myr**, and geological evidence indicates a minor period of $\approx 60 \pm 2$ Myr, from which a polar frequency of **4** for our system may be deduced^[2]. A rough estimate of the observable mass within our radius would therefore be:

$$[14] m_1 + m_2 \approx \frac{1,708,860,759.5^3}{4(240,000,000)^2} \approx 2.17 \times 10^{10} M_{\odot},$$

which eliminates the necessity of dark matter.

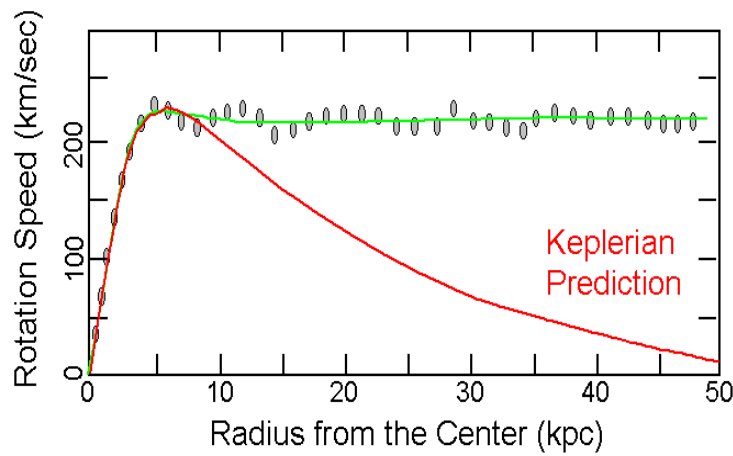


FIG. 11: Assuming $J>1$ as a star's distance increases eliminates the necessity of dark matter.

The angular momenta of celestial systems are volume dependent (VDAM). While the formula $L=T\phi$ is efficient for planets within a solar system, the angular momenta of stellar systems relative to galactic nuclei are more efficiently determined by the stellar formula $L=T\phi_s$, and:

$$[15] \phi_s = \frac{j_s}{2\pi} = \frac{\lambda_s p_s}{2\pi},$$

where λ_s is the stellar wavelength and p_s is the stellar momentum. A temporal phenomenon also emerges from VDM since, according to the Hubble-Lorentz transformation equation:

$$[16] t' = \frac{t - v_D x / c^2}{\sqrt{1 - v_D^2 / c^2}} \propto V_H = (c/H_0)^3$$

where v_D is the volume dependent velocity; our perception of time t is also dependent upon the volume of our inertial frame of reference. In the unified model below, the gray **frame 1** zooms out to the black **frame 2**. **Frame 2** then zooms out to the magenta **frame 3**, etcetera.

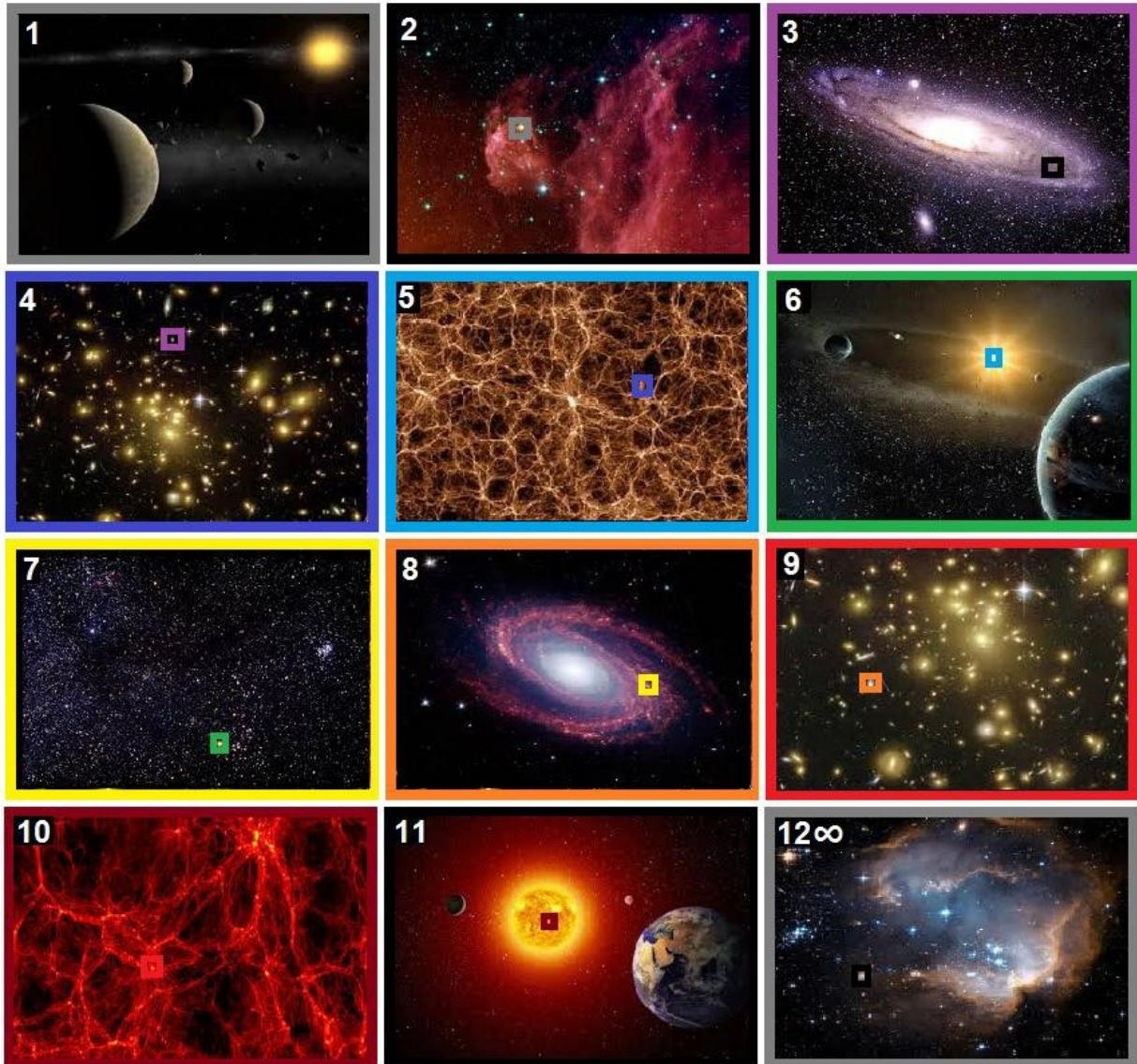
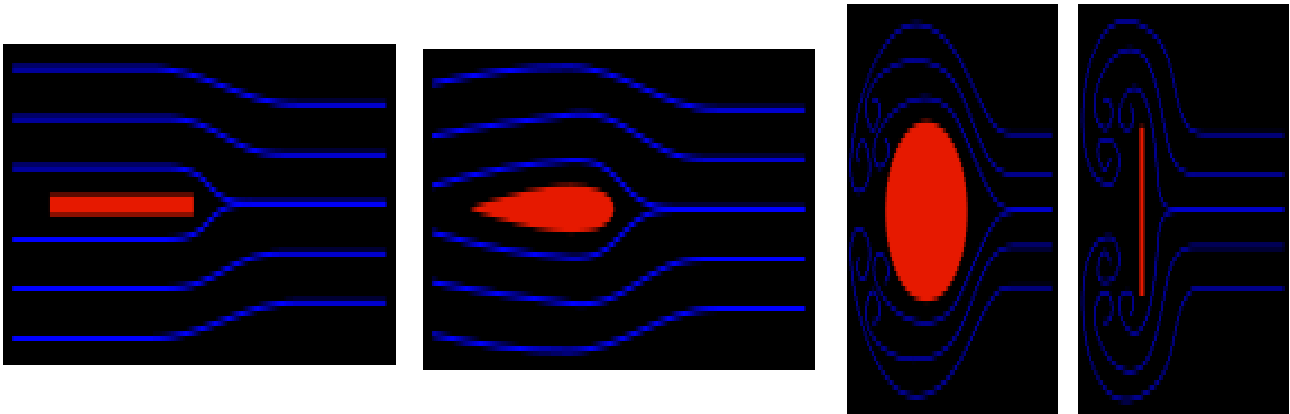


FIG. 12: The Fractal Tesla-Lorentz-Alfvén-Mandelbrot-Einstein (T-FLAME) model of GKD.

In the T-FLAME model, the bandwidth of our Universe is governed by the velocity of light, and there are recursive Hubble-Planck volumes with fractal bandwidths that can be detected via quantum teleportation. Since our perception of time and GEM forces are volume dependent, the model predicts the velocity of quantum teleportation is limited to c^2 (the velocity of the scalar waves (fractal radiation) in **frames 1-6** in **FIG. 12** is c^2 relative to our **frame 11**). While it takes $\approx 100,000$ years for light to travel across the diameter of the Milky Way, it only takes ≈ 122 days for scalar waves, so a very long distance is required in order to detect them. The model can also explain the presence of cosmic microwave background (CMB) radiation without the necessity of a “big-bang” event followed by rapid inflation.

Scalar waves can establish a “positive charge” for black-holes relative to the “negative charge” of luminous bodies since its velocity is far beyond the velocity required to escape their pull (a solution for the black-hole entropy problem). Each galactic nuclei would essentially be a mass producer of scalar waves (dark energy), which can explain our perception of the accelerated expansion of space. Scalar waves can also enable us to communicate on galactic distance scales at the square of the velocity of light, and they may even be utilized as an inexhaustible source of energy (as inferred by Einstein's $E=mc^2$). The technology that can be developed with a basic understanding of GKD is truly revolutionary.

Since the Multiverse is segmented by a hierarchy of recursive Hubble-Planck bandwidths in the FLAME model, each “parallel Universe” can exist in/at the same space-time without interference, except in cases elucidated by Einstein's theory of special relativity.



A body will experience impedance from the recursive Hubble-Planck subsets of the fractal continuum as it is accelerated to relativistically high velocities. Although the mass-energy density of the continuum increases at each subset, the viscosity of the continuum decreases in effect. This allows the continuum to pass through inert matter with infinitesimal resistance and cast neg-entropic shade, but when “inert” matter is accelerated to relativistically high velocities with our conventional means of propulsion it experiences impedance due to an increase in its GM field^[1]. Since we can identify the reason a body is unable to surpass the velocity of light we can theoretically achieve superluminal exploration with GKD.

Acknowledgements

This paper is dedicated to Cindy Lett. It would not have been possible without her.

References within paper:

- [1] P. Marmet, “*Fundamental Nature of Relativistic Mass and Magnetic Fields*,” <http://www.newtonphysics.on.ca/magnetic/> (2013).
- [2] M. R. Rampino and R. B. Stothers, “*Terrestrial mass extinctions, cometary impacts, and the Sun's motion perpendicular to the galactic plane*,” *Nature* 308, 709 – 712 (1984).
- [3] J. C. Hafele and R. E. Keating, “*Around-the-World atomic clocks: Predicted Relativistic Time Gains*,” *Science* 177 (4044): 166-168 (1972).

Important additional references:

- [4] M. Tajmar, F. Plesescu, K. Marhold, and C.J. de Matos, “*Experimental Detection of the Gravitomagnetic London Moment*”, arXiv:gr-qc/0603033v1 (2006).
- [5] P. LaViolette, “*The Electric Charge and Magnetization Distribution of the Nucleon: Evidence of a Subatomic Turing Wave Pattern*,” vixra.org/pdf/0910.0006v1.pdf, (2008).
- [6] M. S. El Naschie and L. Marek-Crnjac, “*Deriving the Exact Percentage of Dark Energy Using a Transfinite Version of Nottale's Scale Relativity*,” *International Journal of Modern Nonlinear Theory and Application*, in Press (2012).
- [7] M. El Naschie, “*Revising Einstein's $E = mc^2$, a Theoretical Resolution of the Mystery of Dark Energy*,” *Proceedings of the Fourth Arab International Conference in Physics and Material Science*, Egypt, 1-3 October, p. 1 (2012).

-
- [8] B. Mandelbrot, "*The fractal geometry of nature*," Macmillan, ISBN 978-0-7167-1186-5 (1983).
- [9] H. Alfvén, "*On hierarchical cosmology*," *Astrophysics and Space Science* (ISSN 0004-640X), vol. 89, no. 2, January 1983, p. 313-324 (1983).
- [10] A. L. Peratt, "*Introduction to Plasma Astrophysics and Cosmology*" *Astrophysics and Space Science*, v. 227, p. 3-1 (1995).
- [11] H. S. Kragh, "*Cosmology and Controversy: The Historical Development of Two Theories of the Universe*," Princeton University Press, 488 pages, ISBN 0-691-00546-X (pp.482-483) (1996).
- [12] O. Klein, "*Arguments concerning relativity and cosmology*," *Science* 171, 339 (1971).